Available at
http://pvamu.edu/aam
Appl. Appl. Math.
ISSN: 1932-9466
Vol. 9, Issue 2 (December 2014), pp. 763-779

Applications and Applied Mathematics:
An International Journal
(AAM)

Effects of Radiation Absorption and Thermo-diffusion on MHD Heat and Mass Transfer Flow of a Micro-polar Fluid in the Presence of Heat Source

J.I. Oahimire
Department of Mathematics
University of Port Harcourt
Port Harcourt, Nigeria.
imumolen@yahoo.co.uk

B. I. Olajuwon
Department of Mathematics
Federal University of Agriculture
Abeokuta, Nigeria.
ishola_1@hotmail.com

Received: October 15, 2012; Accepted: November 25, 2013

Abstract

An analysis of the heat and mass transfer effects on an unsteady flow of a micro-polar fluid over an infinite moving permeable plate in a saturated porous medium in the presence of a transverse magnetic field, radiation absorption and thermo-diffusion were studied. The governing system of partial differential equations was transformed to dimensionless equations using suitable dimensionless variables. The dimensionless equations were then solved analytically using perturbation technique to obtain the expressions for the velocity, micro-rotation, temperature and concentration. With the help of graphs, the effects of the various important parameters such as the translational velocity, micro-rotational velocity, temperature and concentration fields within the boundary layer entering into the problem were discussed. Also the effects of the pertinent parameters on the skin friction coefficient, couple stress coefficient and rates of heat and mass transfer in terms of the Nusselt number and Sherwood numbers were presented numerically in tabular form. The results showed that the observed parameters have a significant influence on the flow, heat and mass transfer.

Keywords: Micro-polar fluid; perturbation technique; heat and mass transfer; heat generation; radiation absorption and thermal radiation

MSC 2010 No.: 76A10, 76V05, 76W05, 74A05, 76S05

1. Introduction

The behavior of fluids that contain suspended metal or dust particles in many practical situations was first observed by Eringen (1966). The coupling between the spin of each particle and the macroscopic velocity fields were taken into account.

Micro-polar fluids are those pertaining to randomly oriented particles suspended in a viscous medium, which can undergo a rotation that can affect the hydrodynamics of the flow, making it a distinctly non-Newtonian fluid. They constitute an important branch of non-Newtonian fluid dynamics where micro-rotation effects as well as micro-inertia are exhibited. The theory of micro-polar fluids originally developed by Eringen (1966) has been a popular field of research in recent years and it has provided a good model for studying a number of complicated fluids, such as colloidal fluids, polymeric fluids and blood.

The effects of radiation on unsteady free convection flow and heat transfer problems have become more important in industries. At high operating temperatures, radiation effects can be quite significant. Many processes in engineering occur at high temperature and knowledge of radiation heat transfer becomes very important for the design of reliable equipment, nuclear plants, gas turbines and various propulsion devices or aircraft, missiles, satellites and space vehicles.

The study of heat generation or absorption effects in moving fluids is important in view of several physical problems, such as fluid undergoing exothermic or endothermic chemical reaction. In certain applications such as those involving heat removal from nuclear fuel debris, underground disposal of radioactive waste material, storage of food stuffs, and exothermic chemical reaction and dissociating fluids in packed-bed reactors, the working fluid for the heat generation or absorption effects are important.

Cogley et al. (1968) showed that in the optically thin limit, the fluid does not absorb its own emitted radiation but the fluid absorbs radiation emitted by the boundaries. Hossain and Takhar (1996) considered the radiation effects on a mixed convection boundary layer flow of an optically dense viscous incompressible fluid along a vertical plate with uniform surface temperature. Makinde (2005) examined the transient free convection interaction with thermal radiation of an absorbing emitting fluid moving along a vertical permeable plate. Satter and Hamid (1966) investigated the unsteady free convection interaction with thermal radiation of an absorbing emitting plate. Rahman and Satter (2007) studied the transient convective flow of a micro-polar fluid past a continuous moving porous plate in the presence of radiation. Heat and mass transfer effects on unsteady magneto hydrodynamics free convection flow near a moving vertical plate embedded in a porous medium was presented by Das and Jana (2010).

Olajuwon (2011) examined convectional heat and mass transfer in a hydro-magnetic flow of a second grade fluid past a semi-infinite stretching sheet in the presence of thermal radiation and thermo diffusion. Haque et al. (2011) studied micro-polar fluid behavior on steady magneto hydrodynamics free convection flow and mass transfer through a porous medium with heat and mass fluxes. Soret and Dufour effects on mixed convection in a non-Darcy porous medium, saturated with micro-polar fluid were studied by Srinivascharya (2011).

Rebhi (2007) studied the unsteady natural convection heat and mass transfer of micro-polar fluid over a vertical surface with constant heat flux. The governing equations were solved numerically using McCormack's technique and effects of various parameters were investigated on the flow. Keelson and Desseaux (2001) studied the effects of surface conditions on the flow of a micro-polar fluid driven by a porous stretching surface. The governing equations were solved numerically. Sunil et al. (2006) studied the effect of rotation on a layer of micro-polar ferromagnetic fluid heated from below saturating a porous medium. The resulting non-linear coupled differential equations from the transformation were solved using a finite-difference method.

Mahmoud (2007) investigated thermal radiation effects on magneto hydrodynamic flow of a micro-polar fluid over a stretching surface with variable thermal conductivity. The solution was obtained numerically using the Runge–Kutta fourth order method. Reena and Rana (2009) investigated double-diffusive convection in a micro-polar fluid layer heated and soluted from below in a saturating porous medium. A linear stability analysis theory and normal mode analysis method was used. Kandasamy et al. (2005) studied the nonlinear MHD flow, with heat and mass transfer characteristics, of an incompressible, viscous, electrically conducting, Boussinesq fluid on a vertical stretching surface with chemical reaction and thermal stratification effects. Seddek (2005) studied the effects of chemical reaction, thermo-pharoses and variable viscosity on a steady hydromagnetic flow with heat and mass transfer over a flat plate in the presence of heat generation/absorption. Patil and Kulkarni (2008) studied the effect of chemical reaction on the flow of a polar fluid through a porous medium in the presence of internal heat generation. Double-diffusive convection radiation interaction on unsteady MHD flow over a vertical moving porous plate with heat generation and Soret effects was studied by Mohamed (2009). Khedr et al. (2008) studied MHD flow of a micro-polar fluid past a stretched permeable surface with heat generation or absorption. Unsteady free convection in non-Newtonian fluids has many applications in geophysics; turbo-machinery and many other fields. Chaudhary and Abhay (2008) studied the effect of chemical reactions on MHD micro-polar fluid flow past a vertical plate in slip-flow regime.

Modather et al. (2009) studied MHD heat and mass transfer flow of a micro-polar fluid over a vertical permeable plate in a porous medium without considering the effects of thermal radiation, heat generation and thermo diffusion. Motivated by these applications and previous work done, we studied the effects of thermal radiation, heat generation, thermo diffusion and radiation absorption on an unsteady free convection heat and mass transfer flow of a micro-polar fluid past a vertical porous plate. The governing equations are solved analytically using the perturbation method and the effect of various physical parameters were discussed numerically and graphically

2. Mathematical Formulation

We consider a two-dimensional non-Darcian mixed convection flow of a viscous, incompressible, electrically conducting micro-polar fluid over an infinite vertical porous moving permeable plate in a saturated porous medium. A magnetic field of strength B_0 is applied perpendicular to the surface and the effect of the induced magnetic field is neglected. The x^*-axis is taken along the planar surface in the upward direction and the y^*- axis taken to be normal to it as shown in Figure 1. Due to the infinite plane surface assumptions, the flow variables are

function of y^* and t^* only. Initially, the fluid as well as the plate is at rest, but for time $t > 0$ the whole system is allowed to move with a constant velocity. At $t = 0$, the plate temperature is suddenly raised to T_w.

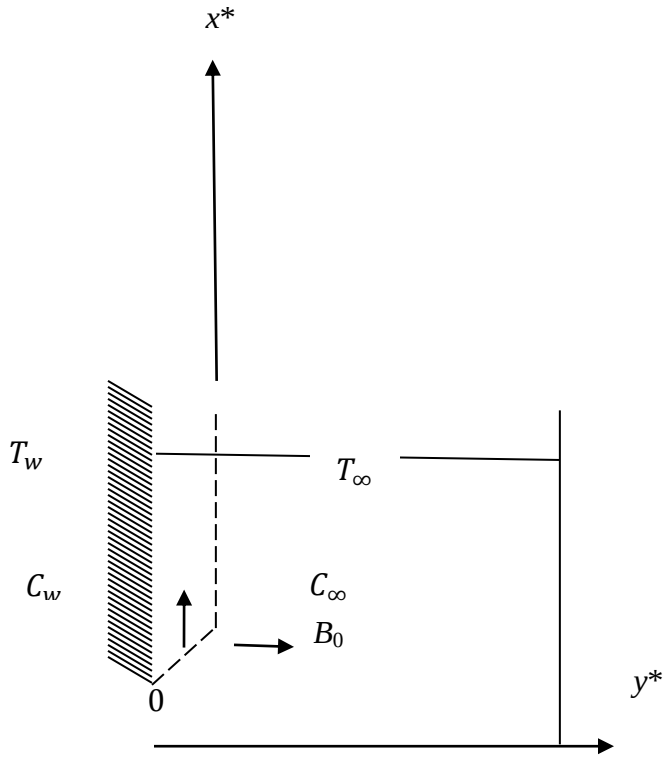

Figure 1: Physical model

The governing equations for the motion are given by

$$\frac{\partial u^*}{\partial y^*} = 0, \tag{1}$$

$$\frac{\partial u^*}{\partial t^*} + v^* \frac{\partial u^*}{\partial y^*} = (\nu + \nu_r)\frac{\partial^2 u^*}{\partial y^{*2}} + 2\nu_r \frac{\partial w^*}{\partial y^*} + g\beta_T(T - T_\infty)$$

$$+ g\beta_c(C - C_\infty) - \sigma \frac{B_0^2 u^*}{\rho} \frac{\nu + \nu_r}{K} u^*, \tag{2}$$

$$\rho J^* \left(\frac{\partial w^*}{\partial t^*} + v^* \frac{\partial w^*}{\partial y^*}\right) = \gamma \frac{\partial^2 w^*}{\partial y^{*2}}, \tag{3}$$

$$\frac{\partial T}{\partial t^*} + v^* \frac{\partial T}{\partial y^*} = \alpha \frac{\partial^2 T}{\partial y^{*2}} - \frac{1}{\rho C_p} \frac{\partial q_r}{\partial y^*} + \frac{Q_0 (T - T_\infty)}{\rho C_p} + Q_1^* (C - C_\infty)$$

$$+ \frac{DK_t}{C_s C_p}, \tag{4}$$

$$\frac{\partial C}{\partial t^*} + v^* \frac{\partial C}{\partial y^*} = D \frac{\partial^2 C}{\partial y^{*2}}, \tag{5}$$

where (u^*, v^*) are the components of the velocity at any point (x^*, y^*), w* is the component of the angular velocity normal to (x^*, y^*) plane, T is the temperature of the fluid and C is the mass concentration of the species in the flow. $\rho, v, v_r, g, \beta_T, \beta_c, \sigma, K, j^*, \gamma, \alpha, D, K_t, Q_0, C_s, Q_1^*$ and C_p are the density, kinematic viscosity, kinematic rotational viscosity, acceleration due to gravity, coefficient of volumetric thermal expansion of the fluid, coefficient of volumetric mass expansion of the fluid, electrical conductivity of the fluid, permeability of the medium, micro-inertia per unit mass, spin gradient viscosity, thermal diffusivity, molecular diffusivity thermal diffusion ratio, constant heat flux per unit, concentration susceptibility, coefficient of proportionality of the radiation and specific heat at constant pressure respectively.

The appropriate boundary conditions for the problem are

$$\begin{aligned} &u^* = u_p^*, \;\; w^* = -n_1 \frac{\partial u^*}{\partial y^*}, \\ &T = T_\infty + \varepsilon (T_w - T_\infty) e^{n^* t^*}, \\ &C = C_\infty + \varepsilon (C_w - C_\infty) e^{n^* t^*} asy^* = 0, \\ &u^* \to 0, w^* \to 0, T \to T_\infty, C \to C_\infty asy^* \to \infty. \end{aligned} \tag{6}$$

ε is a scalar constant far less than unity. The following comments should be made about the boundary condition used for the micro-rotation term; When $n_1 = 0$, $w^* = 0$. This represents the case of concentrated particle flows in which the microelements close to the wall are unable to rotate [Jena and Mathur (1982)]. The case corresponding to $n_1 = 0.5$ results in the vanishing of the anti- symmetric part of the stress tensor and represent weak concentration. Ahmadi (1976) suggested that the particle spin is equal to the fluid vorticity at the boundary for fine particle suspension. As suggested by Peddieson (1972), the case corresponding to n_1=1 is representative of turbulent boundary layer flows. Thus, for n_1=0, the particle are not free to rotate near the surface. However, as $n_1 = 0.5$ and 1, the micro-rotation term gets augmented and induces flow enhancement.

Integrating equation (1), we get

$$u^* = -V_0, \tag{7}$$

where, V_0 is a scale of suction velocity, which has a non-zero positive constant.

Following Rosseland approximation [Brewstar (1972)] the radiative heat flux q_r is modeled as

$$q_r = \frac{4\sigma^*}{3k^*} \frac{\partial T^4}{\partial y^*}, \tag{8}$$

where σ^* is the Stefan-Boltzmann constant and k^* is the mean absorption coefficient. Assuming that the difference in temperature within the flow is such that T^4 can be expressed as a linear combination of the temperature, we expand T^4 in Taylor's series about T_∞ as follows:

$$T^4 = T_\infty^4 + 4T_\infty^3(T - T_\infty) + 6T_\infty^2(T - T_\infty)^2 + \cdots \tag{9}$$

and neglecting higher order terms beyond the first degree in$(T - T_\infty)$, we have

$$T^4 \approx -3T_\infty^4 + 4T_\infty^3 T. \tag{10}$$

Differentiating equation (8) with respect to y* and using equation (10) to obtain

$$\frac{\partial q_r}{\partial y^*} = \frac{-16T_\infty^3\sigma^*}{3k*}\frac{\partial^2 T}{\partial y^{*2}}. \tag{11}$$

We introduce the following dimensionless variables:

$$u = \frac{u^*}{U_0}, v = \frac{v^*}{V_0}, y = \frac{V_0 y^*}{\nu}, U_p = \frac{u_p^*}{U_0}, w = \frac{\nu}{U_0 V_0}w^*, t = \frac{t^* V_0^2}{\nu},$$

$$\theta = \frac{T-T_\infty}{T_w-T_\infty}, \phi = \frac{C-C_\infty}{C_w-C_\infty}, n = \frac{n^*\nu}{V_0^2},\ J = \frac{V_0^2 J^*}{\nu^2},\ \ \eta = \frac{\mu J^*}{\gamma} = \frac{2}{2+\beta}. \tag{12}$$

Substituting equation (12) into equations (2) – (5) yield the following dimensionless equations:

$$\frac{\partial u}{\partial t} - \frac{\partial u}{\partial y} = (1+\beta)\frac{\partial^2 u}{\partial y^2} + 2\beta\frac{\partial w}{\partial y} + Gr\theta + Gc\phi - Mu - \frac{1+\beta}{K'}u, \tag{13}$$

$$\frac{\partial w}{\partial t} - \frac{\partial w}{\partial y} = \frac{1}{\eta}\frac{\partial^2 w}{\partial y^2}, \tag{14}$$

$$\frac{\partial \theta}{\partial t} - \frac{\partial \theta}{\partial y} = \frac{1}{Pr}(1+Nr)\frac{\partial^2 \theta}{\partial y^2} + H\theta + Q_1\phi + Df\frac{\partial^2 \phi}{\partial y^2}, \tag{15}$$

$$\frac{\partial \phi}{\partial t} - \frac{\partial \phi}{\partial y} = \frac{1}{Sc}\frac{\partial^2 \phi}{\partial y^2}, \tag{16}$$

where,

$M = \frac{\sigma B_0^2 \nu}{\rho V_0^2}$ is the magnetic field parameter, $Gr = \frac{\nu\beta_T g(T_w-T_\infty)}{U_0 V_0^2}$ is the Grashof number,

$Gc = \frac{\nu\beta_c g(C_w-C_\infty)}{V_0^2 U_0}$ is the modified Grashof number, $Pr = \frac{\nu}{\alpha} = \frac{\nu\rho C_p}{K}$ is the Prandtl number,

$Sc = \frac{\nu}{D}$ is the Schmidt number, $H = \frac{\nu Q_0}{\rho C_p V_0^2}$ is the heat source parameter,

$Df = \frac{DK_t(C_w-C_\infty)}{C_s C_p \nu(T_w-T_\infty)}$ is the Dufour number, $Nr = \frac{16T_\infty^3\sigma^*}{3K^*K}$ is the thermal radiation parameter, $K' = \frac{KU_0V_0^2}{\nu^2}$ is the permeability parameter, $\beta = \frac{\nu_r}{\nu}$ is the dimensionless viscosity ratio (where ν_r and ν are kinematic rotational viscosity and kinematic viscosity respectively) and $Q_1 = \frac{\nu Q_1^*(C_w-C_\infty)}{V_0^2(T_w-T_\infty)}$ is the radiation absorption parameter.

The corresponding boundary conditions are

$$u = U_p, \qquad \theta = 1 + \varepsilon e^{nt},$$

$$w = -n_1 \frac{\partial u}{\partial y},\ \phi = 1 + \varepsilon e^{nt} at y = 0,$$

$$u \to 0,\ w \to 0,\ \theta \to 0,\ \phi \to 0\ as\ y \to \infty. \tag{17}$$

3. Method of Solution

To find the analytical solution of the above system of partial differential equations (13) – (16) subject to the boundary conditions (17), we assume a perturbation of the form:

$$u = u_0(y) + \varepsilon e^{nt} u_1(y) + o(\varepsilon^2), \tag{18}$$
$$w = w_0(y) + \varepsilon e^{nt} w_1(y) + o(\varepsilon^2), \tag{19}$$
$$\theta = \theta_0(y) + \varepsilon e^{nt} \theta_1(y) + o(\varepsilon^2), \tag{20}$$
$$\phi = \phi_0(y) + \varepsilon e^{nt} \phi_1(y) + o(\varepsilon^2), \tag{21}$$

Substituting equations (18) – (21) into equations (13) - (16), neglecting the higher order terms of $O(\varepsilon^2)$ to obtain the following set of equations:

$$(1+\beta)u_0'' + u_0' - C_1 u_0 = -Gr\theta_0 - Gc\phi_0 - 2\beta w_0', \tag{22}$$

$$(1+\beta)u_1'' + u_1' - C_2 u_1 = -Gr\theta_1 - Grc\phi_1 - 2\beta w_1', \tag{23}$$

$$w_0'' + \eta w_0' = 0, \tag{24}$$

$$w_1'' + \eta w_1' - \eta n w_1 = 0, \tag{25}$$

$$a\theta_0'' + \theta_0' + H\theta_0 + Q_1\phi_0 + Df\phi_0'' = 0, \tag{26}$$

$$a\theta_1'' + \theta_1' + (H-n)\theta_1 + Q_1\phi_1 + Df\phi_1'' = 0, \tag{27}$$

$$\phi_0'' + Sc\phi_0' = 0, \tag{28}$$

$$\phi_1'' + Sc\phi_1' - Scn\phi_1 = 0, \tag{29}$$

where,

$$a = \frac{Pr}{1+Nr}, C_1 = M + \frac{1+\beta}{K'}, C_2 = n + M + \frac{1+\beta}{K'}.$$

The corresponding boundary conditions can be written as

$$u_0 = U_p,\ u_1 = 0, w_0 = -n_1 u_0',\ w_1 = -n_1 u_1',$$

$$\theta_0 = 1,\ \theta_1 = 1, \phi_0 = 1, \phi_1 = 1\ ,$$

$$u_0 = 0, u_1 = 0, w_0 = 0, w_1 = 0, \theta_0 = 0,$$

$$\theta_1 = 0, \phi_0 = 0, \phi_1 = 0\ at\ y \to \infty. \tag{30}$$

The solution of (22) - (29) satisfying the boundary conditions (30) are given by

$$u = A_1 e^{-m_2 y} + A_2 e^{-m_1 y} + A_3 e^{-Scy} + A_4 e^{-\eta y} + (A_5 e^{-m_6 y} + A_6 e^{-m_4 y} + A_7 e^{-m_3 y} + A_8 e^{-m_5 y}) \varepsilon e^{nt}, \quad (31)$$

$$w = B_1 e^{-\eta y} + \varepsilon e^{nt} B_2 e^{-m_5 y}, \quad (32)$$

$$\theta = D_1 e^{-m_2 y} + D_2 e^{-Scy} + \varepsilon e^{nt} (D_3 e^{-m_4 y} + D_4 e^{-m_3 y}), \quad (33)$$

$$\phi = e^{-Scy} + \varepsilon e^{nt} e^{-m_3 y}, \quad (34)$$

where,

$$m_1 = \frac{1+\sqrt{1+4aH}}{2a}, m_2 = \frac{1+\sqrt{1+4(1+\beta)C_1}}{2(1+\beta)}, m_3 = \frac{Sc+\sqrt{Sc^2+4nSc}}{2},$$

$$m_4 = \frac{1+\sqrt{1-4a(H-n)}}{2a}, m_5 = \frac{\eta+\sqrt{\eta^2+4\eta n}}{2}, m_6 = \frac{1+\sqrt{1+4(1+\beta)C_1}}{2(1+\beta)},$$

$$D_2 = \frac{-(Q_1+DfSc^2)}{aSc^2-Sc+H}, D_1 = 1 - D_2, A_2 = \frac{-GrD_1}{(1+\beta)m_1^2-m_1-C_1},$$

$$A_3 = \frac{-(GrD_2+Gc)}{(1+\beta)Sc^2-Sc-C_1}, A_4 = \frac{2\beta\eta n_1(m_2U_p-m_2A_2-m_2A_3+m_1A_2+ScA_3)}{((1+\beta)\eta^2-\eta-C_1)+2\beta\eta n_1(m_2-\eta)}$$

$$A_1 = U_p - A_2 - A_3 - A_4, \quad B_1 = n_1(m_2A_1 + m_1A_2 + ScA_3 + \eta A_4),$$

$$D_4 = \frac{-(Q_1+Dfm_3^2)}{am_3^2-m_3+(H-n)}, D_3 = 1 - D_4, A_6 = \frac{-GrD_3}{(1+\beta)m_4^2-m_4-C_2},$$

$$A_7 = \frac{-(GrD_4+Gc)}{(1+\beta)m_3^2-m_3-C_2}, A_8 = \frac{2\beta m_5 n_1(m_4A_6+m_3A_7-m_6A_6-m_6A_7)}{\left((1+\beta)m_5^2-m_5-C_2\right)+2\beta m_5 n_1(m_6-m_5)},$$

$$A_5 = -(A_6 + A_7 + A_8), B_2 = n_1(m_6A_5 + m_4A_6 + +m_3A_7 + m_5A_8).$$

4. Results

The results are presented as velocity, micro-rotation, temperature and concentration profiles in Figures 2 – 19 below:

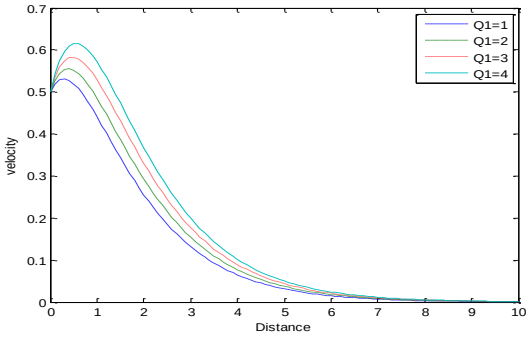

Figure 2. Velocity profiles for different values of radiation absorption parameter

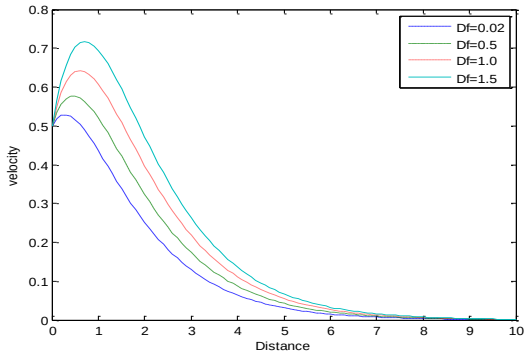

Figure 3. Velocity profiles for different values of Dufour number

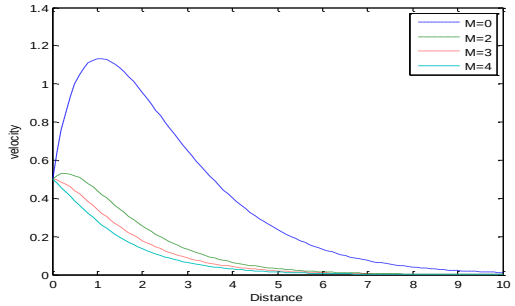

Figure 4. Velocity profiles for different values of magnetic field parameter

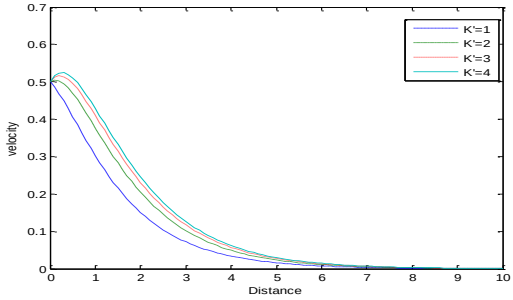

Figure 5. Velocity profiles for different values of permeability parameter

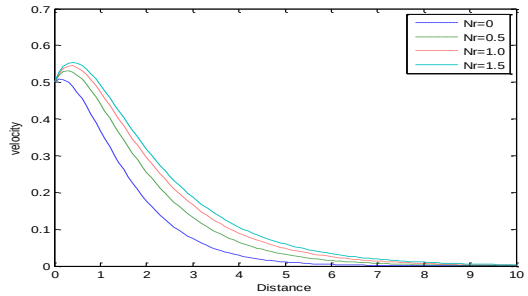

Figure 6. Velocity profiles for different values of radiation parameter

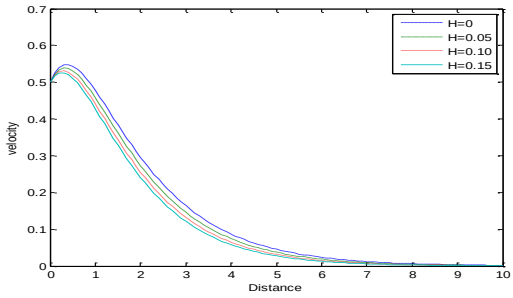

Figure 7. Velocity profiles for different values of heat source parameter

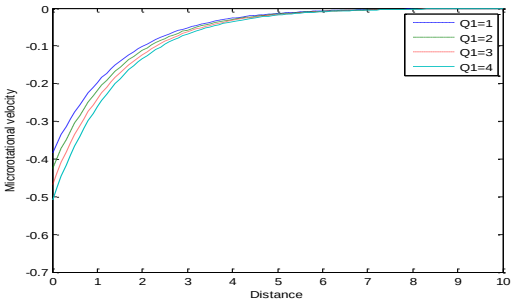

Figure 8. Micro-rotation profiles for different values of radiation absorption parameter

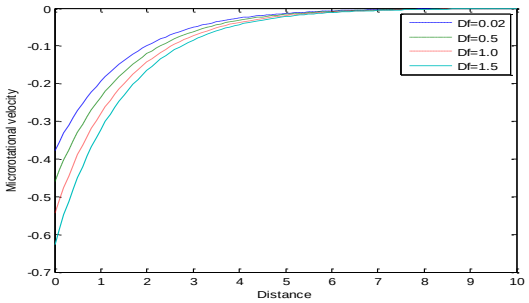

Figure 9. Micro-rotation profiles for different values of Dufour number

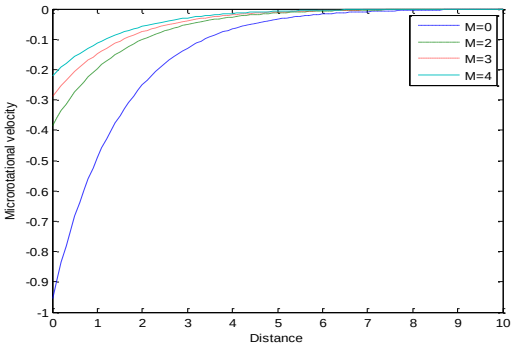

Figure 10. Micro-rotation profiles for different values of magnetic field parameter

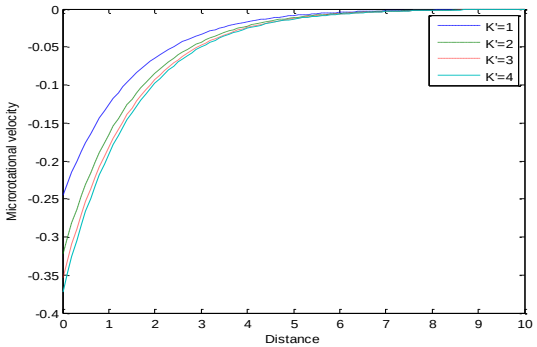

Figure 11. Micro-rotation profiles for different values of permeability parameter

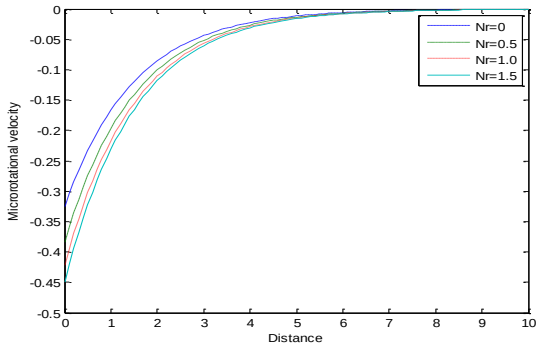

Figure 12. Micro-rotation profiles for different values of radiation parameter

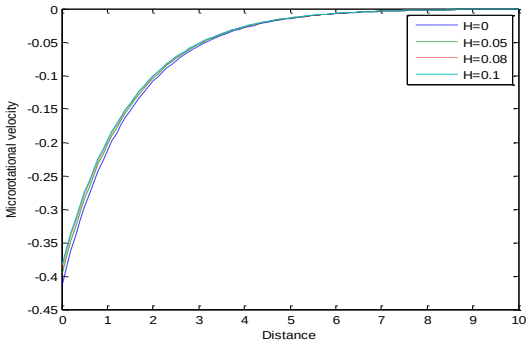

Figure 13. Micro-rotation profiles for different values of heat source parameter

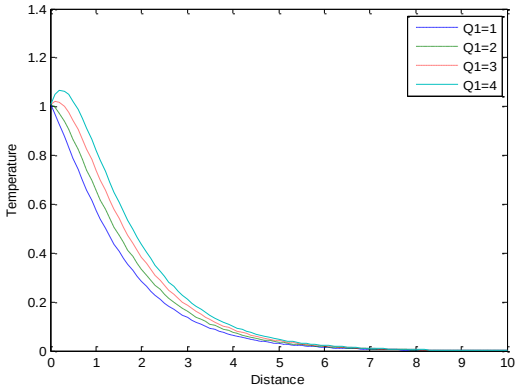

Figure 14. Temperature profiles for different values of radiation absorption parameter

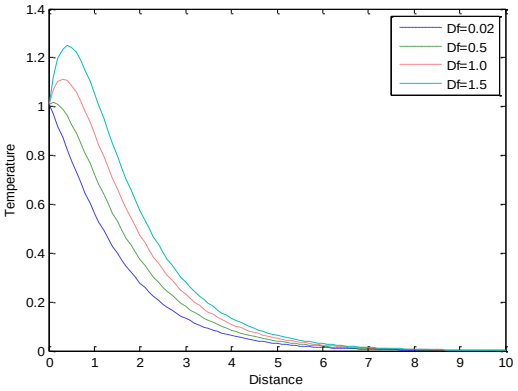

Figure 15. Temperature profiles for different values of Dufour number

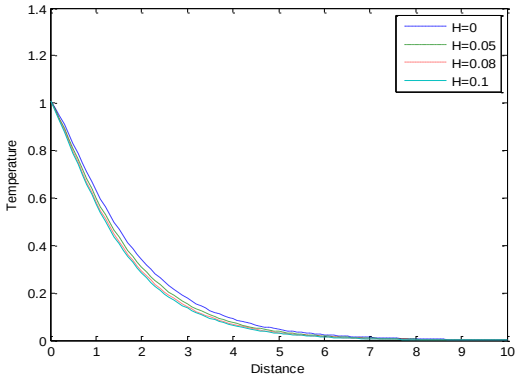

Figure 16. Temperature profiles for different values of heat source parameter

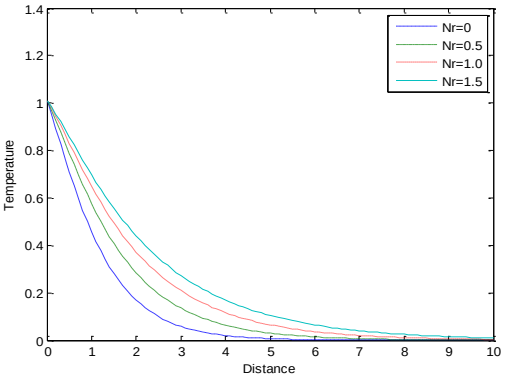

Figure 17. Temperature profiles for different values of radiation parameter

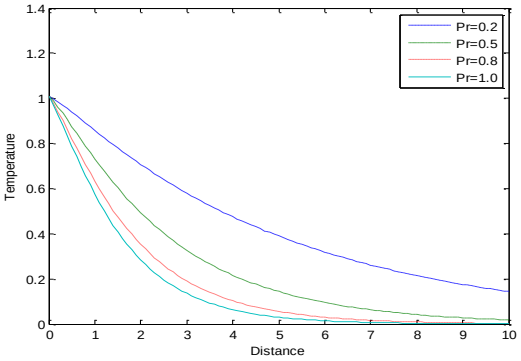

Figure 18. Temperature profiles for different values of Prandtl number

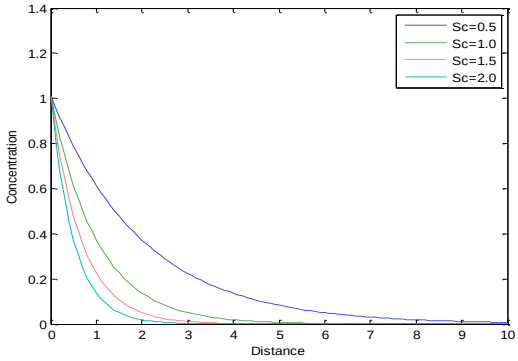

Figure 19. Concentration profiles for different values of Schmidt number

The local skin friction coefficient, couple stress coefficient, Nusselt number and Sherwood number are important physical quantities of engineering interest. The skin friction coefficient (C_f) at the wall is given by

$$C_f = \frac{2\tau_w}{\rho U_0 V_0} = 2[1 + (1 - n_1)\beta]u'(0)$$
$$= -2[1 + (1 - n_1)\beta][m_2 A_1 + m_1 A_2 + ScA_3 + \eta A_4 + \varepsilon e^{nt}(m_6 A_5 + m_4 A_6 + m_3 A_7 + m_4 A_8), \quad (35)$$

where, τ_w^* is the wall shear stress.

The couple stress coefficient (C_w') at the plate is written as;

$$C_w' = \frac{M_w \nu^2}{\mu U_0 V_0^2} = w'(0) = -(\eta B_1 + \varepsilon e^{nt} B_2 m_5). \quad (36)$$

The rate of heat transfer at the surface in terms of the Nusselt number is given by;

$$Nu = \frac{x(\frac{\partial T}{\partial y^8})}{(T_\infty - T_w)},$$
$$NuRe_x^{-1} = -\theta'(0)$$
$$= m_1 D_1 + ScD_2 + \varepsilon e^{nt}(m_4 D_3 + m_3 D_4), \quad (37)$$
$$Re_x = \frac{xV_0}{\nu}.$$

The rate of mass transfer at the surface in terms of the local Sherwood number is given by

$$Sh = \frac{(\frac{\partial c}{\partial y^*})_{y^*=0}}{C_\infty - C_w},$$

$$ShRe_x^{-1} = -\phi'(0) = Sc + \varepsilon e^{nt} m_3. \quad (38)$$

The numerical result for skin friction coefficient, couple stress coefficient, Nusselt number, Sherwood number and unsteady behaviour of the coefficients of skin friction, couple stress coefficient, heat transfer and mass transfer with various values of time are shown in Tables 1–4.

Table 1. Effect of *Q1, Df, H, Sc* and *Nr* parameter on C_f and C'_w with $\varepsilon = 0.01$, $n = 0.1$, $n_1=0.5$, $\beta=1$, $Gr=2$, $Gc=1$, $M=2$, $Pr=1$, $t=1$, $K'=5$, $Up=0.5$

Q1	*Df*	*Sc*	*Nr*	*H*	C_f	C'_w
1.0	0.05	2.0	0.5	0.1	0.7239	0.0810
2.0	0.05	2.0	0.5	0.1	0.9753	0.1090
3.0	0.05	2.0	0.5	0.1	1.2266	0.1369
1.0	0.02	2.0	0.5	0.1	0.6937	0.0776
1.0	0.5	2.0	0.5	0.1	1.1769	0.1314
1.0	1.0	2.0	0.5	0.1	1.6801	0.1874
1.0	0.05	0.5	0.5	0.1	18.8513	2.0955
1.0	0.05	1.0	0.5	0.1	1.3284	0.1483
1.0	0.05	1.5	0.5	0.1	0.9849	0.1100
1.0	0.05	2.0	0.5	0.1	0.7239	0.0810
1.0	0.05	2.0	1.0	0.1	0.9558	0.1068
1.0	0.05	2.0	1.5	0.1	1.1229	0.1254
1.0	0.05	2.0	0.5	0.05	0.8065	0.0902
1.0	0.05	2.0	0.5	0.08	0.7554	0.0845
1.0	0.05	2.0	0.5	0.1	0.7239	0.0810

Table 2. Effect of *Q1, Df, H, Pr* and *Nr* parameter on $NuRe_x^{-1}$ with $\varepsilon = 0.01$, $n=0.1$, $n_1=0.5$, $\beta=1$, $Gr=2$, $Gc=1$, $M=2$, $Sc=1$, $t=1$, $K'=5$, $Up=0.5$

Q1	*Df*	*Pr*	*Nr*	*H*	NuRe_x^{-1}
1.0	0.05	1.0	0.5	0.1	0.3937
2.0	0.05	1.0	0.5	0.1	0.0865
3.0	0.05	1.0	0.5	0.1	-0.2207
1.0	0.02	1.0	0.5	0.1	0.4306
1.0	0.5	1.0	0.5	0.1	-0.1599
1.0	1.0	1.0	0.5	0.1	-0.7749
1.0	0.05	0.5	0.5	0.1	0.2270
1.0	0.05	0.8	0.5	0.1	0.3261
1.0	0.05	1.0	0.5	0.1	0.3937
1.0	0.05	1.0	0.5	0.1	0.3937
1.0	0.05	1.0	1.0	0.1	0.3094
1.0	0.05	1.0	1.5	0.1	0.2599
1.0	0.05	1.0	0.5	0.05	0.3359
1.0	0.05	1.0	0.5	0.08	0.3713
1.0	0.05	1.0	0.5	0.1	0.3937

Table 3. Effect of Sc parameter on $ShRe_x^{-1}$ with $n=0.1$, $\varepsilon=0.01$, $n_1=0.5$, $\beta=1$, $Gr=2$, $Gc=1$, $M=2$, $Up=0.5$, $t=1$, $Q1=1$, $Pr=1$, $H=0.1$, $Df=0.05$ and $K'=5$

Sc	$ShRe_x^{-1}$
0.5	0.5065
1.0	1.0121
1.5	1.5176

Table 4. Unsteady behavior of the coefficient of skin-friction, couple stress coefficient, heat transfer and mass transfer with various value of t when $\varepsilon=0.01$, $n=0.1$,$n_1=0.5$, $\beta=1$, $Gr=2$,$Gc=1$, $M=2$, $Pr=1$, $Q1=1$,$Df=0.05$, $H=0.1$, $Sc=2$, $K'=5$ and $Up=0.5$.

T	C_f	$C'w$	$NuRe_x^{-1}$	$ShRe_x^{-1}$
0	0.7203	0.0805	0.3934	2.0210
1	0.7239	0.0810	0.3937	2.0232
3	0.7324	0.0821	0.3943	2.0283
5	0.7427	0.0834	0.3952	2.0345
10	0.7798	0.0880	0.3981	2.0570
20	0.9415	0.1084	0.4112	2.1548
30	1.3812	0.1637	1.4465	2.4209

5. Discussion

Numerical evaluation of the analytical solutions reported in the previous section was performed. The results were presented in graphical and tabular form. This was done to illustrate the influence of the various parameter involved. In this study, we have chosen $\varepsilon=0.01$, $n=0.1$, $\beta=1$ and $Up=0.5$ while t, $Q1$, Df, H, Nr, Pr, K' and M are varied over a range.

Figure 2 shows the velocity profiles for different values of the radiation absorption parameter $Q1$. As the radiation absorption parameter increases, the velocity profiles increase and we observe that an increase in the value of absorption of radiation parameter due to increase in the buoyancy force will accelerate the flow rate.

Figure 3 illustrates the variation of the velocity profiles with different values of thermo-diffusion parameter (or Dufour number) Df. The velocity profiles increase with an increase in the Dufour number. The effect of increasing the value of the Dufour number is to increase the boundary layer thickness.

The effects of the magnetic field parameter on the velocity distribution profiles across the boundary layer are presented in Figure 4. It is obvious that the effect of increasing values of the magnetic field parameter M is a decreasing in the velocity distribution across the boundary layer. This is due to the fact that the introduction of transverse magnetic field normal to the flow direction causes the tendency to create a drag force due to Lorentz force and hence results in retarding the velocity profiles.

Figure5 depicts the effect of the permeability parameter(K') on the velocity distribution profiles from which it becomes obvious that as the permeability parameter(K') increases, the velocity increases along the boundary layer thickness which is expected since when the holes of porous medium become larger, the resistivity of the medium may be neglected.

Figure 6 illustrates the effect of the thermal radiation parameter on the velocity distribution profiles. As it can be seen from the figure, the velocity profiles increases with an increase in the thermal radiation parameter (Nr) and as a result, the momentum boundary layer thickness increases. This is because an increase in the intensity of heat generated through thermal radiation increased weakens, the bond holding the components of the fluid particle is and the fluid velocity.

Figure 7 shows that an increase in the heat generation parameter decreases the velocity profiles. Figure 8 shows the variation of the micro-rotational velocity distribution profiles with different

values of radiation absorption parameter. It is clear from the figure that an increase in the radiation absorption decreases the micro-rotational velocity. Figure 9 shows the influence of Dufour number in the micro-rotation profiles. The micro-rotational velocity profiles decreases as the Dufour number increases.

Figure 10 depicts the micro-rotational velocity profiles for different values of the magnetic field parameter *(M)*. In contrast to the velocity distribution profiles, the micro-rotational velocity distribution increases with an increase in the magnetic field parameter. The effect due to the permeability parameter (*K')* on the micro-rotational velocity is shown in Figure 11. It is observed that as permeability parameter increases, the micro-rotational velocity decreases.

Figure 12 illustrates the micro-rotational velocity distribution for different values of radiation parameter (*Nr)*; the figure shows that as radiation parameter increases, micro-rotational velocity decreases. Figure13 shows that the effect of increasing the heat generation parameter is to increase the micro-rotational velocity.

Figure 14 depicts the variation of the temperature profiles with different values of radiation absorption parameter. It is seen from this figure that the effect of the absorption of radiation parameter is to increase the temperature in the boundary layer as the radiated heat is absorbed by the fluid which in turn increases the temperature of the fluid very close to the porous boundary layer and its effect diminishes far away from the boundary layer. Figure 15 shows the influence of the Dufour number on the temperature profile. The temperature of the fluid an increases with increase in Dufour number.

Figure16 presents the temperature profiles for various values of the heat source parameter. It is obvious from the figure that an increase in the heat source parameter decreases the fluid temperature. Figure17 presents temperature distribution profiles for different values of the radiation parameter. It is clear from the figure that the temperature profiles increase as the radiation parameter increases and hence there would be an increase of the thermal boundary layer thickness.

Figure 18 presents the effect of the Prandtl number Pr on the temperature profiles. Increasing the values of Pr has the tendency to decrease the fluid temperature in the boundary layer as well as the thermal boundary-layer thickness. This causes the wall slope of the temperature to decrease as the Pr increases causing the Nusselt number to increase as can be clearly seen in Table 2.

Figure 19 shows the concentration distribution profiles for different values of the Schmidt number. It can be noted from the figure that the concentration of the fluid decreases as the Schmidt number increases. Table 1 shows the effect of *Q1, Df, H, Sc* and *Nr* on the skin friction coefficient, C_f and couple stress coefficient. It is observed that the increase in *Q1, Df* and Nr increases the skin friction coefficient while increase in Sc and H decrease the skin friction coefficient. Increase in *Q1, Df* and *Nr* increases the couple stress coefficient while increase in *Sc* and *H* decreases the couple stress coefficient.

Table 2 shows the effect of *Q1, Df* and *Sc* on the Nusselt number. The Nusselt number increases with the increase in *Pr* and *H*. This shows that the surface heat transfer from the porous plate increases with the increasing values of the *Pr*. And the *Nu* decreases with increase in *Nr, Q1* and

Df. Table 3 indicates the effect of *Sc* on the Sherwood number *Sh*. It is clear from the table that as Sc increases, the Sherwood number increases.

Table 4 illustrates the variation of the coefficients of the skin friction, couple stress coefficient, heat transfer and mass transfer with various value of *t*. It can be seen that the skin friction coefficient, couple stress coefficient, heat transfer and mass transfer an increase with time. These results are in excellent agreement with the result of Chaudhary and Abhay (2008) and Modather et al. (2009).

6. Conclusion

We studied the MHD heat and mass transfer of the laminar flow of an incompressible, electrically conducting micro-polar fluid over an infinite vertical moving plate in a saturated porous medium. The resulting partial differential equations which describe the problem are transformed to dimensionless equations using dimensionless variables. We then solve the equations analytically by using the perturbation technique. The results are discussed through graphs and tables for different values of parameters entering the problem.

The following conclusions can be drawn from the results obtained:

- The radiation absorption increases the translational velocity and temperature in the boundary layer while it decreases the micro-rotational velocity.

- In the presence of a uniform magnetic field, an increase in the strength of the applied magnetic field decelerates the fluid motion along the wall of the plate inside the boundary layer, whereas the micro-rotational velocity of the fluid along the wall of the plate increases.

- The increase in the thermal radiation parameter increases the momentum and thermal boundary layer thickness while it decelerates micro-rotational velocity.

- The Nusselt number increases as the Prandtl number and the heat source increase and decreases as the radiation parameter, absorption parameter and Dufour number increase.

- The Sherwood number increases as the Schmidt number increases.

REFERENCE

Ahmadi, G. (1976). Self-similar solution of incompressible micro-polar boundary layer flow over a semi-infinite plate, Int. J. Eng. Sci., 14, pp. 639-648.

Brewster, M.Q. (1972). Thermal radiation transfer properties, John Wiley and Sons, 12, pp. 6-9.

Chaudhary, R.C. and Abhay, K.J. (2008). Effect of chemical reaction on MHD micro-polar fluid flow past a vertical plate in slip-flow regime. Appl. Math. Mech. Engl. Ed. 29(9), pp. 117-134.

Cogley, A.C., Vincent W.E. and Gilles, S.E. (1968). Differential approximation for radiation in a non-gray gas near equilibrium, AIAAJ. 6, pp. 551-553.

Das, K. and Jana, S. (2010). Heat and mass transfer effects on unsteady MHD free convection flow near a moving vertical plate in a porous medium. Bull. Soc. Banjaluka, 17, pp.15-32.

Erigen A.C (1966). Theory of micro-polar fluids. J. Math. Mech. 16, pp.1-18

Ganapathy, R. (1994). A note on oscillatory coquette flow in a rotating system. ASME J. Appl. Mech. 61, pp. 208-209.

Haque, M.D.Z., Alam, M.D. M., Ferdows, M. and Postelnicu, A. (2011). Micro-polar fluid behaviors on steady MHD free convection flow and mass transfer with constant heat and mass fluxes, joule heating and viscous dissipation. J. King Saud Univ. Eng. Sci. doi:10.1016/j.jksues.2011.02.003.

Hossain, M.A., Takhar, H. (1996). Radiation effect on mixed convection along a vertical plate with uniform surface temperature, Heat mass transfer, 31, pp. 243-248

Jena, S.K. and Mathur, M.N. (1982). Free convection in the laminar boundary layer flow of a thermo micro-polar fluid past a vertical flat with suction/injection, Acta Mechanica, 42, pp. 216-227.

Kandasamy, R., Periasamy, K. and Sivagnana, K. (2005). Chemical reaction, heat and mass transfer on MHD flow over a vertical stretching surface with heat source and stratification effects, Int. J. of Heat and Mass Transfer, 48, pp.45-57.

Keelson, N.A., Desseaux, A. (2001). Effects of surface condition on flow of a micro-polar fluid driven by a porous stretching sheet, Int. J. Eng. Sci, 39, pp. 1881-1897.

Khedr M.E., Chamkha A.J. and Bayomi, M. (2008). MHD flow of a micro-polar fluid past a stretched permeable surface with heat generation or absorption, Non-linear analysis modeling and control, 14, pp. 27-40.

Mahmoud, M.A (2007). Thermal radiation effects on MHD flow of a micro-polar fluid over a stretching surface with variable thermal conductivity. Physical A. 375, pp. 401-410

Makinde, O.D. (2005). Free convection flow with thermal radiation and mass transfer past a moving vertical porous plate. Int. Comm. Heat Mass Transfer, 25, pp.289-295.

Modather M, Rashad A.M, Chamkha A.J (2009). Study of MHD heat and mass transfer of oscillatory flow of a micro-polar fluid over a vertical permeable plate in a porous medium. Turkish J. Zeng. Env. Sci., 33, pp. 245-257.

Olajuwon, B.I. (2011). Convection heat and mass transfer in a hydro-magnetic flow of a second grade fluid in the presence of thermal radiation and thermal diffusion, Int. comm. Heat and mass, 38, pp. 377-382.

Patil, P.M. and Kulkarni, P.S. (2008). Effects of chemical reaction on free convective flow of a polar fluid through a porous medium in the presence of internal heat generation, Int. Therm. Sci. 4. pp. 1043-1054.

Peddieson, J. (1972). Boundary layer theory for a micro-polar fluid, Int. J. Eng. Sci., 10, 23-29.

Rahman, M.A. and Satter, M.A. (2007). Transient convective flow of micro-polar fluid past a continuously moving vertical porous plate in the presence of radiation. International Journal of Applied Mechanics and Engineering, Vol. 12, pp. 497-513.

Rawat, S. and Bhargava, R. (2009). Finite element study of natural convection heat and mass transfer in a micro-polar fluids - saturated porous regime with Soret/Dufour effects. Int. J. of Appl. Maths and Mech., 5(2), pp. 58-71.

Reena I. and Rana U.S. (2009). Linear stability of thermo solutal convection in a micro-polar fluid saturating a porous medium, International Journal of Application and Applied mathematics, 4, pp. 62-87.

Rees, D.A and Bassom, A.P. (1996). The Blasius boundary layer flow of micro-polar fluid, Int. Eng. Sci, 34, pp. 113-124.

Rehbi, A.D., Tariq, A.A., Benbella, A.S. Mahmoud, A.A. (2007). Unsteady natural convection heat transfer of micro-polar fluid over a vertical surface with constant Heat flux, Turkish J. Eng. Env. Sci., 31, pp. 225-233.

Satter, M.D.A. and Hamid M.D.K. (1966). Unsteady free convection interaction with thermal radiation in a boundary layer flow past a vertical porous plate. Jour. Math. Phys. Sci., 30, pp. 25-37.

Seddek, M.A. (2005). Finite-element method for effects of chemical reaction, variable viscosity, thermophoresis and heat generation/absorption on a boundary layer hydromagnetic flow with heat and mass transfer over a heat surface, Acta mech., 177, pp. 1-18.

Srinivasachanya. D., Ramreddy. C.H. (2011). Soret and Dufour effect on mixed convection in a non-Darcy porous medium saturated with micro-polar fluid, Non-analysis modeling and control, Vol. 16, No.1, pp. 100-115.

Sunil, A., Sharma, A., Bharti, P.K. and Shandi, R.G. (2006). Effect of rotation on a layer of micro-polar ferromagnetic fluid heated from below saturating a porous medium. Int. J. Eng. Sc., 44, pp. 683-698.